Available online at www.sciencedirect.com
ScienceDirect
Journal of Nuclear Materials 358 (2006) 69–76
journal of nuclear materials
www.elsevier.com/locate/jnucmat

Behaviour of chromium steels in liquid Pb–55.5Bi with changing oxygen content and temperature

Alfons Weisenburger [a,*], Kazumi Aoto [b], Georg Müller [a], Annette Heinzel [a], Gustav Schumacher [a], Tomohiro Furukawa [b]

[a] *Forschungszentrum Karlsruhe GmbH, Institut für Hochleistungsimpuls und Mikrowellentechnik, Hermann-von-Helmholtz-Platz 1, 76344 Eggenstein-Leopoldshafen, Germany*
[b] *O-arai Engineering Center, Japan Atomic Energy Agency (JAEA), Japan*

Received 24 May 2006; accepted 4 July 2006

Abstract

The behaviour of protective oxide layers on P122 steel and its welds and of ODS steel in liquid $Pb_{44.5}Bi_{55.5}$ (LBE) is examined under conditions of changing temperatures and oxygen concentrations. P122 (12Cr) and its welded joints are exposed to LBE at 550 °C for 4000 h with oxygen concentrations of 10^{-6} and 10^{-8} wt% ($p(O_2) = 8.1 \times 10^{-23}$ bar and 5.2×10^{-27} bar) which change every 800 h. It is found that like in case of constant oxygen concentration of 10^{-6} wt% a protective spinel layer ($(Fe(Fe_{1-x}Cr_x)_2O_4)$) was maintained on P122 and also on its welded joint. Two experiments with exposure times of 4800 h are conducted on ODS steel, both with temperatures changing from 550 to 650 °C and back every 800 h, one experiment with 10^{-6} the other with 10^{-8} wt% oxygen in LBE. Both experiments show strong local dissolution attack after 4800 h which is in agreement with the behaviour of ODS in LBE at a constant temperature of 650 °C. However, dissolution attack is less in LBE with 10^{-8} wt% oxygen ($p(O_2) = 3.0 \times 10^{-25}$ bar).

1. Introduction

$Pb_{44.5}Bi_{55.5}$ – lead bismuth eutectic (LBE) – is a candidate material for the coolant of a fast breeder reactor (FBR). One of the main problems in the development of such a system is the compatibility of the steels with LBE.

In 1998 experiments were reported in which oxide scales formed on the surface of austenitic steels protected the steel from dissolution attack by flowing LBE [1]. For stabilization of these oxide scales a controlled concentration of dissolved oxygen in LBE has to be maintained. The concentration applied in the experiments was 10^{-6} wt%. Recent work on corrosion of austenitic and martensitic steels gives an overview on the corrosion effects and processes and its prevention in stagnant and flowing Pb and LBE [2–11]. However, few data only were presented on the reactions taking place in LBE with different oxygen concentrations and

* Corresponding author. Tel.: +49 7247 82 6238; fax: +49 7247 82 2256.
E-mail address: alfons.weisenburger@ihm.fzk.de (A. Weisenburger).

0022-3115/$ - see front matter © 2006 Elsevier B.V. All rights reserved.
doi:10.1016/j.jnucmat.2006.07.001

also at temperatures above 550 °C. Experiments with ODS exposed for 5000 h to stagnant LBE with 10^{-4} and 10^{-8} wt% oxygen showed no dissolution attack up to 650 °C while at 10^{-6} wt% attack was observed [12]. Tests with aluminized coatings on 316L and T91 steels in LBE with oxygen concentrations $<10^{-8}$ wt% showed satisfying protection of the steel only up to 500 °C but severe dissolution attack at 600 °C already after 1000 h [13].

The work reported so far deals with the steel attack observed at different constant temperatures and oxygen concentrations. It is, however, important to know the behaviour of steels under conditions of changing temperatures and oxygen concentrations which can be expected during the course of reactor operation. The present paper describes the effect of temperature variations at different constant oxygen concentrations in LBE for ODS steel. The influence of changing oxygen concentration, which can happen due to loss of oxygen situations, is examined on P122 steel and also on welded joints of this material. Both steels are candidate materials for the fuel cladding of a LBE-cooled FBR.

2. Experimental

2.1. Materials

The compositions of ODS steel and of P122 steel and its solder used in the experiments are given in Table 1. The specimens are plates of $28 \times 8 \times 2\ mm^3$ dimension.

The welded joints of two pieces of P122 are made using the TIG process applying a solder the composition of which is very similar to that of P122. Fig. 1 shows the cross-section of the joint and the structures that appear in and around the weld. The weld exhibits a coarse-grained structure. It is separated from the bulk of the joint steel by a heat-affected fine grained zone of 1.2 cm thickness. No significant variation of the composition is found for the different zones.

2.2. Control of oxygen concentration in LBE

The experiments are conducted in the COSTA device [2] in which the specimens are exposed to stagnant LBE under conditions of temperature and oxygen concentration fluctuations, respectively. The control of oxygen concentrations is obtained in this device via the gas phase by establishing the corresponding oxygen partial pressure via the H_2/H_2O ratio in the gas flowing through the furnace tubes [2]. Variation of oxygen concentration is attained by changing the H_2/H_2O ratio in the flowing gas every 800 h. Temperature variations are realized by changing the heating power of the furnace also every 800 h.

Table 1
Composition of ODS steel and of P122 steel and its solder (in wt%)

Element	ODS[a]	P122	Solder
C	0.13	0.11	0.09
Si	<0.005	0.27	0.3
Mn	<0.01	0.64	0.52
P	0.001	0.016	0.005
S	0.003	0.002	0.002
Ni	0.01	0.33	1.04
Cu	–	1.0	1.51
Cr	8.85	10.54	10.5
W	1.94	1.76	1.43
Ti	0.2	–	–
Mo	–	0.34	0.26
Y	0.27	–	–
O	0.17	–	–
Nb + Ta	–	0.048	0.05
N	0.011	0.071	0.0424
V	–	0.19	0.2
Ar	0.005	–	–

[a] Heat treatment: 1050 °C – 1 h (AC); 800 °C – 1 h (AC).

The influence of changes in the LBE temperature and of the oxygen potential in the gas phase on the oxygen concentration in LBE can be revealed by looking at the Ellingham diagram [14] in Fig. 2, which contains the lines of constant oxygen concentrations in LBE and Pb based on measurements for Pb [15] and LBE [16] and also those obtained from our calculations for LBE [14].

H_2/H_2O equilibrium ratios are represented by dashed thin lines ascending with temperature and oxygen concentrations in LBE and Pb by solid and dashed thick lines descending with temperature. We refer in our considerations to the solid concentration lines which correspond to our calculations [14] for LBE. The points on the lines mark the conditions of the experiments described in the following sections.

The diagram shows that the oxygen concentration in LBE decreases when the temperature is reduced at constant H_2/H_2O ratio. Oxygen is removed from LBE by equilibration of the oxygen dissolved in LBE with the H_2/H_2O ratio in the gas phase. The oxygen concentration in LBE decreases

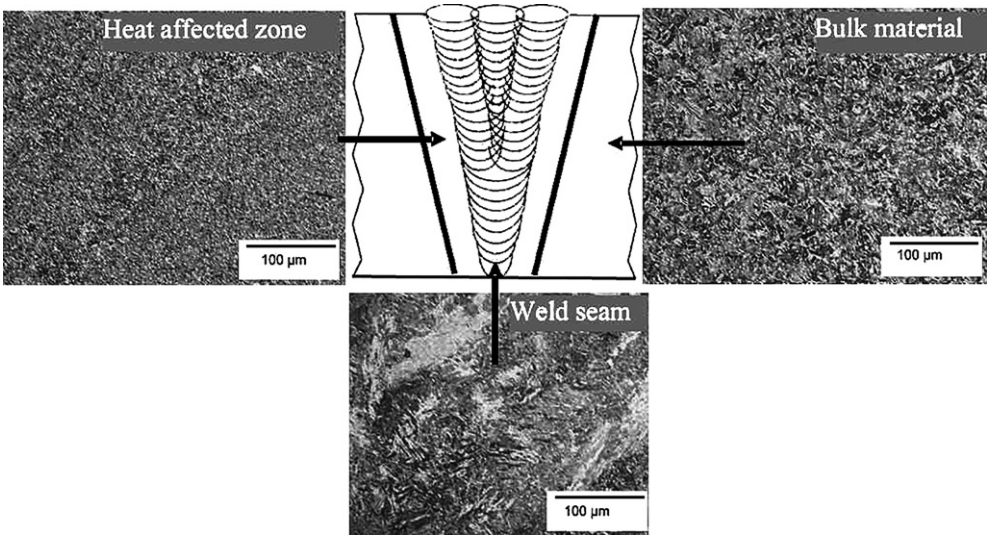

Fig. 1. Scheme of the welded joins and structures of the zones that appear.

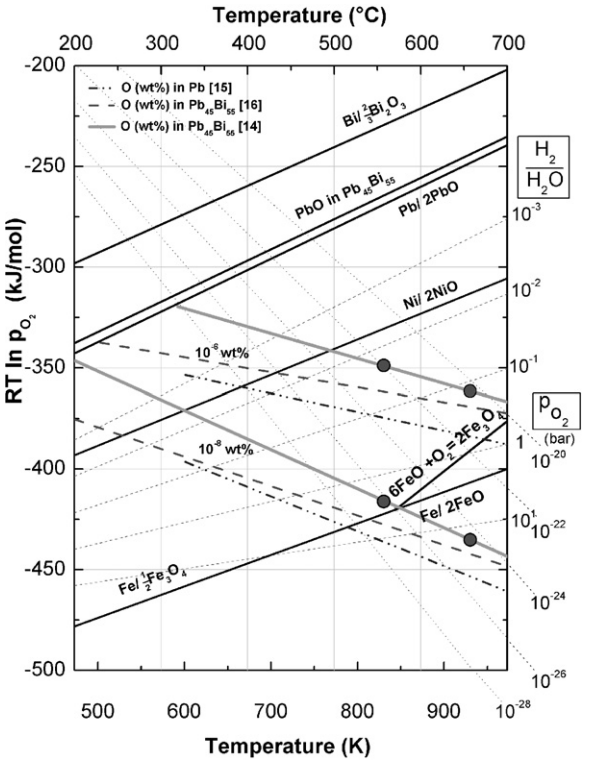

Fig. 2. Ellingham diagram with lines of constant oxygen concentrations in LBE and Pb [14] according to data from Risold [15] for Pb and from measurements by Gromov, Orlov, et al. [16] and our calculations [14] for LBE.

also by the same process when the H_2/H_2O ratio increases at constant temperature.

The lowest oxide formation line in this diagram is that for the enthalpy of formation of wustite (FeO) and below 570 °C that of magnetite (Fe_3O_4) [17]. Above this line a magnetite and wustite scale develop on the surface by diffusion of iron into this scale and subsequent oxidation [18]. Below the Fe_3O_4/FeO line magnetite and wustite are not stable any more. However, in Fe–Cr steels with more than 3 wt% a Cr spinel of type $Fe(Fe_{1-x}Cr_x)_2O_4$ develops below the surface by diffusion of oxygen [2,11]. Below the line where dissociation of Fe_3O_4 into $FeO + O_2$ starts spinel formation is observed without FeO formation when the Cr content exceeds 8 wt% [19] like in the materials described in this paper. With the help of tracer diffusion measurements it is shown by Töpfer et al. [20] that the Fe ion diffusion coefficient decreases by up to two orders of magnitude with increasing Cr content in the spinel for low oxygen activities in which the diffusion is governed by cation interstitials.

2.3. Temperature variations

Temperature variations are obtained in the system ODS–LBE by changing the temperature from 550 to 650 °C and back after periods of 800 h up to an exposure time of 4800 h as shown in Fig. 3. Because of the thermal capacity of the furnace the change in temperature is not abrupt. The step from 550 to 650 °C takes 25 min, the step back 100 min. The oxygen concentration was kept constant at

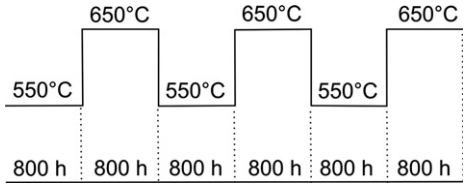

Fig. 3. Temperature as a function of time for ODS in LBE.

Table 2
Oxygen concentrations in LBE and corresponding H_2/H_2O ratios and oxygen partial pressures in the gas phase at different temperatures

c_O (wt%)	550 °C		650 °C	
	H_2/H_2O	$p(O_2)$ (bar)	H_2/H_2O	$p(O_2)$ (bar)
10^{-6}	1.6×10^{-2}	8.1×10^{-23}	1.09×10^{-1}	3.9×10^{-21}
10^{-8}	1.84	5.20×10^{-27}	12.25	3.0×10^{-25}

10^{-6} and 10^{-8} wt%, respectively, by changing the H_2/H_2O ratio in the gas phase according to Table 2.

A critical situation occurs by increasing the temperature to 650 °C along the line of constant oxygen concentration of 10^{-8} wt%, because Fe_3O_4 is not stable any more after this step, see Fig. 2.

2.4. Oxygen concentration variations

Variations of oxygen concentration in LBE are simulated by changing the concentration from 10^{-6} to 10^{-8} wt% and back after periods of 800 h up to an exposure time of 4000 h (Fig. 4). In parallel to the variations experiment specimens were exposed at constant oxygen concentration of 10^{-6} wt% for comparison. The temperatures in the experiments are kept constant at 550 °C. Fig. 2 shows how the different oxygen concentrations in LBE are obtained. It needs a change of the H_2/H_2O ratio by about two orders of magnitude to switch from 10^{-6} to 10^{-8} wt% oxygen and back. The values of oxygen concentrations in LBE and the equilibrium H_2/H_2O ratios and oxygen partial pressures in the gas phase at 550 °C can be obtained from Table 2.

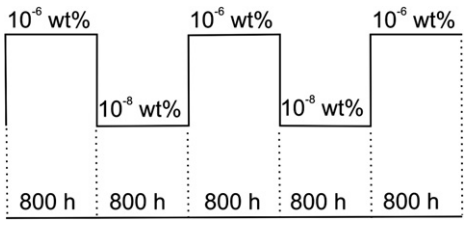

Fig. 4. Oxygen concentration in LBE as a function of time for P122 and its welded joints.

2.5. Evaluation

The specimens taken out of the COSTA device after the experiments are cut using a diamond disk saw perpendicular to the exposed surface and are grinded and polished for metallographic examinations. Light optical (LOM) and scanning electron (SEM) microscopy (S-800, Hitachi) are employed for observation of the microstructure of the material and the oxide scale. The identification of the phases is supported by energy dispersive X-ray analysis (EDX, WINEDS Thomson Scientific).

3. Results

3.1. Temperature variation between 550 and 650 °C, ODS steel

3.1.1. 10^{-6} wt% Oxygen in LBE

The oxide layer on the specimen after 2400 h constitutes of spinel, clearly indicated by the existence of Cr in the layer as shown in the concentration profile, see Fig. 5. No magnetite is found on the top of it. Small quantities of spalled-off magnetite are found floating on the PbBi surface in the crucible.

The formed spinel layer is rather porous with inclusions of PbBi but protects the whole surface. Bigger pores are located mainly near the interface between spinel layer and bulk material. The highest Cr concentration is measured near the interface. The Cr concentration ranges between 11 and 30 wt% and increases in direction to the interface (see Fig. 5(b)). A diffusion zone (internal oxidation) is not visible. The oxide scale does not spall off during the temperature variations up to 2400 h.

After 4800 h severe localized dissolution attack is observed at few places where the spinel scale spalled off. The dissolution attack concerns two spots on one of the two specimens examined after 2400 h and one area on one of the two specimens exposed for 4800 h, see Fig. 6.

3.1.2. 10^{-8} wt% Oxygen in LBE

ODS specimens exposed to LBE with 10^{-8} wt% of oxygen for 2400 h show now visible oxide scale. It is not clear from Fig. 7 whether a very thin oxide layer prevents the specimen. The holes below the

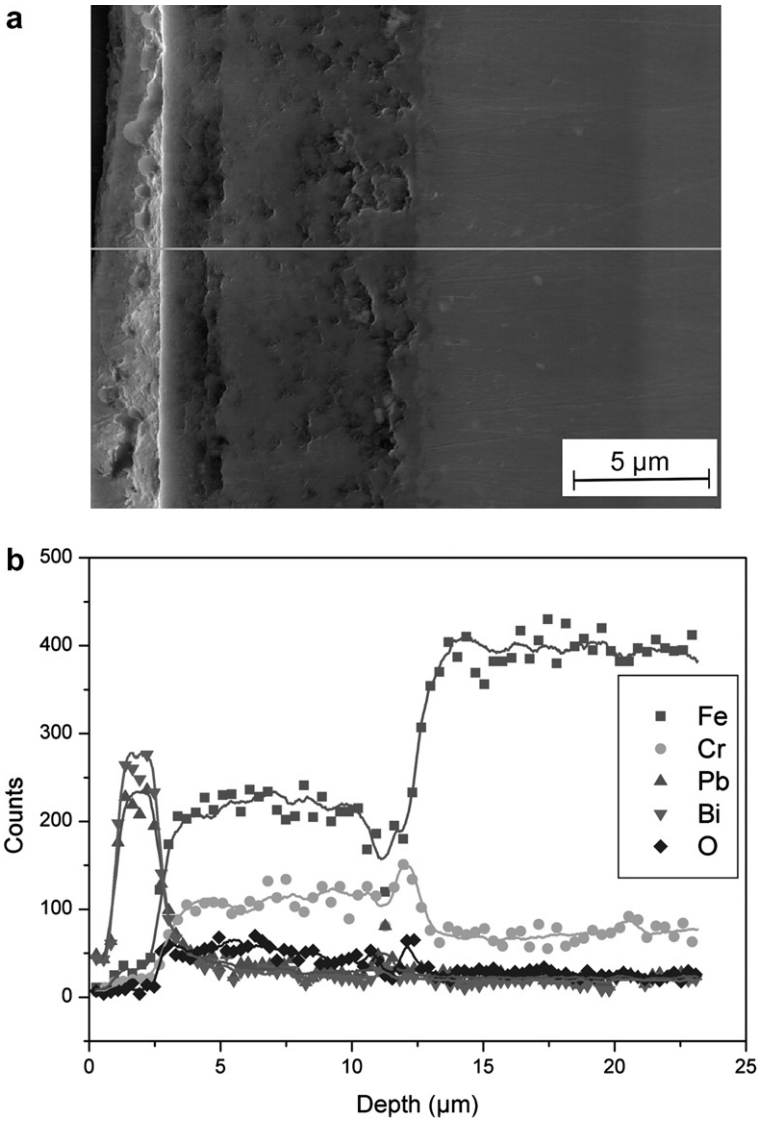

Fig. 5. SEM of ODS surface cross-section after exposure to LBE with 10^{-6} wt% oxygen for 2400 h at temperatures changing from 550 to 650 °C and back every 800 h (a), EDX across surface region (b).

surface at positions where inclusions are broken out during preparation and belong to a zone slightly depleted in Cr, see Fig. 7(b).

The situation changes between 2400 and 4800 h. Two kinds of corrosion phenomena are observed after exposure to LBE with 10^{-8} wt% oxygen and temperature changes between 550 and 650 °C. Part of the surface exhibits local dissolution attack with no visible oxide scale formation in areas of several 100 µm diameter. The attack is enhanced in surface parts where Cr is depleted by carbide formation. The other part still has a protective Cr spinel layer on top with an oxygen diffusion layer underneath which is sealed against the steel by a Cr rich diffusion barrier.

3.2. Variation of oxygen concentration between 10^{-6} and 10^{-8} wt%, P122 steel

3.2.1. Bulk material and welded joint, 550 °C

A dense magnetite and spinel layer develops after 4000 h of exposure on the P122 surface during the experiments with oxygen concentration variations, see Fig. 8. On the bulk material and heat-affected zone the layers (spinel + internal oxidation) are of almost constant thickness (14 µm) while on the weld

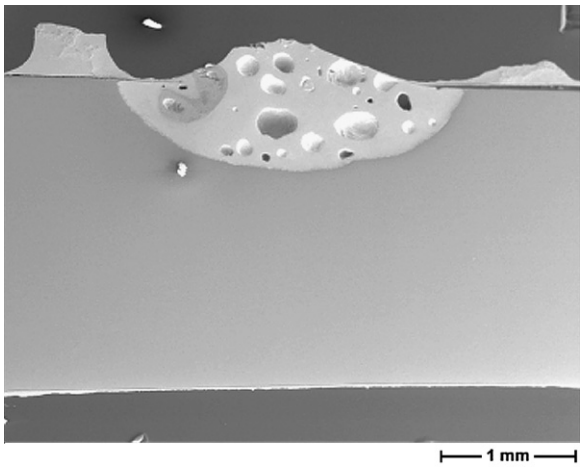

Fig. 6. SEM of ODS surface cross-section after exposure to LBE with 10^{-6} wt% oxygen for 4800 h at temperatures changing from 550 to 650 °C and back every 800 h, part of specimen with strong dissolution attack (LBE in corroded area).

seam the thickness varies along the surface. The Cr content in the spinel layer reaches 20 wt%. LBE penetrates the magnetite layer, precipitates in the interface to the spinel layer and separates the magnetite layer.

Parallel to the experiment with variation of the oxygen concentration a second experiment with constant oxygen concentration at 10^{-6} wt% was conducted for comparison at the same temperature of 550 °C. The result is shown in Fig. 9.

The appearance of the oxide scales formed with constant oxygen concentration is similar to that shown in Fig. 8. However, the magnetite scale in Fig. 9 has higher porosity. The spinel and internal oxidation zone are of larger thickness (24 μm). Its spinel zone contains less amount of Cr, about 16 wt%. The magnetite layer is not separated but contains LBE in its pores.

4. Discussion

Spinel oxide scales without magnetite develop on ODS under conditions of temperatures changing between 550 and 650 °C every 800 h. This behaviour agrees with results observed in the CORRIDA loop experiments [21] in which the oxygen concentration changed to lower values during the course of the experiment. This agreement is not surprising, because increasing temperature and decreasing oxygen content have both the effect of decreasing the oxygen activity which hinders the formation of a magnetite scale, as can be seen from Fig. 1. An internal spinel layer develops instead of this as already described by Müller et al. [2]. The spinel layer prevents the ODS steel from dissolution attack as long as no spallation occurs. This agrees also with former experiments with ODS at a constant temperature of 550 °C and 10^{-6} wt% oxygen concentration ($p(O_2) = 8.1 \times 10^{-23}$ bar) up to 2000 h of exposure [12]. At an oxygen concentration of 10^{-6} wt% the spinel layer is relatively thick, while at 10^{-8} wt% ($p(O_2) = 5.2 \times 10^{-27}$ bar) only a thin spinel layer is formed. Local dissolution attack occurs on ODS steel after the exposure for 4800 h in LBE with 10^{-6} and 10^{-8} wt% oxygen at temperatures changing between 550 and 650 °C. This is in contradiction to the observation of prevention of dissolution attack on ODS in LBE with 10^{-8} wt% oxygen ($p(O_2) = 3.0 \times 10^{-25}$ bar) at 650 °C [12]. However, the dissolution attack is less severe in LBE with 10^{-8} wt% oxygen. The attack starts in areas of depleted Cr concentration in which protective spinel formation does not take place any more. The pores observed below the surface are originated by Cr oxicarbide particles that break out during grinding. Defects in the spinel layer that may be caused by the temperature fluctuations cannot be repaired because of the low Cr concentrations in these regions. In areas protected by an intact spinel layer a Cr enrichment at the spinel/bulk interface takes place which forms an effective diffusion barrier. Thus, further spinel growth and internal oxidation are prevented in these areas because of substantial decrease of the iron ion mobility [20].

The P122 specimen tested under loss of oxygen control conditions, simulated by variation of the oxygen concentration between 10^{-6} and 10^{-8} wt% at 550 °C is protected by a stable spinel layer like the one tested at 10^{-6} wt% oxygen at 550 °C. In both specimens Pb–Bi penetrates the magnetite layer. However, the allocation of LBE after the experiments is different. In the specimen exposed to LBE with constant 10^{-6} wt% oxygen the precipitates distribute in more or less fine pores inside the magnetite, while in the specimen with changing oxygen concentration LBE is precipitated just between magnetite layer and spinel. In this case the magnetite layer appears denser and does not allow formation of LBE inclusions in it, but is almost entirely detached from the spinel layer which, however, keeps still its protective function. The reason for incorporation of Pb into the pores of the magnetite layer at constant oxygen concentration of 10^{-6} wt% in LBE is not fully understood. Formation

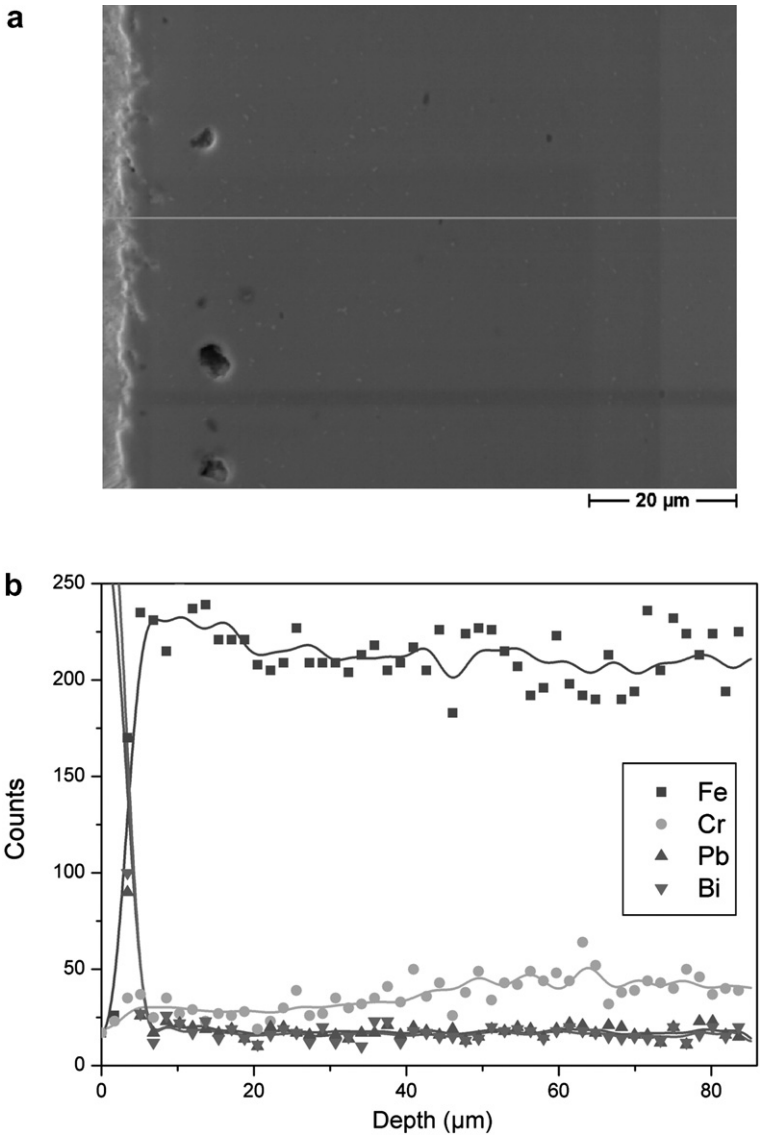

Fig. 7. SEM of ODS surface cross-section after exposure to LBE with 10^{-8} wt% oxygen for 2400 h at temperatures changing from 550 to 650 °C and back every 800 h (a), EDX across surface region (b).

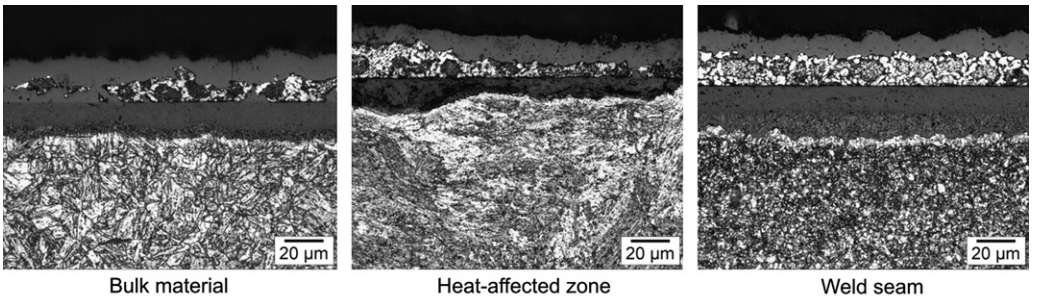

Fig. 8. LOM of the oxide scale on the different zones in the welded joint with oxygen concentrations in LBE changing from 10^{-6} to 10^{-8} wt% every 800 h at 550 °C.

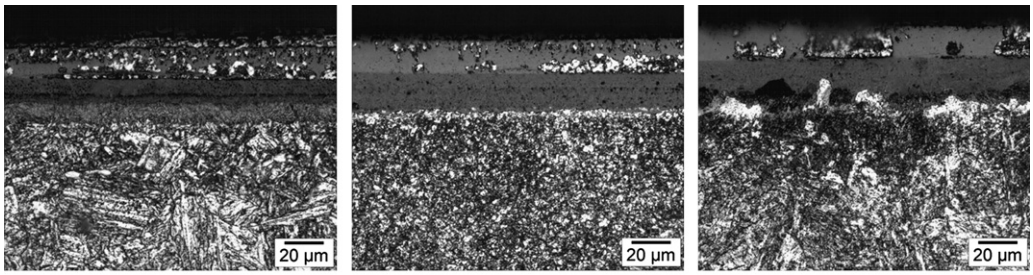

Fig. 9. LOM of the oxide scale on the different zones in the welded joint with constant oxygen concentration of 10^{-6} wt% in LBE at 550 °C.

of a thin layer of Pb–Fe oxides on the magnetite may change the wetting properties of LBE. This may lead to the inclusion of Pb during the magnetite growth. Pb–Fe oxides are not expected to be formed at 10^{-8} wt% oxygen and 650 °C.

Three different grain structures are observed in welded P122 joints. The finest grains appear in the transition zone between the welding and bulk material. The welded joint is a typical coarse-grained martensitic structure. The grain size of the bulk material is in between the both described structures. Despite this, the structures of the different oxide zones after exposure to LBE with changing oxygen concentration are very similar with the exception of the oxide layer thickness variations above the weld seam which is caused by the coarse grains of this zone.

5. Conclusion

The hot spot simulation experiments in the ODS–LBE system show that dissolution attack cannot be prevented at 650 °C, even though the formation of a protective oxide layer took place before at 550 °C. However, dissolution attack is less severe in LBE with 10^{-8} wt% oxygen. The experiments with changing oxygen concentrations in the P122–LBE system show that such variations do not impose a serious problem on the steel corrosion by LBE at a temperature of 550 °C. Welded joints of P122 are covered with protective oxide layers as well as the original steel surface.

References

[1] I.V. Gorynin, G.P. Karzov, V.G. Markov, V.S. Lavrukhin, V.A. Yakovlev, in: Proceedings of the Conference HLMC 98, Obninsk: SSC RF-IPPE, vol. 1, 1999, p. 120.
[2] G. Müller, G. Schumacher, F. Zimmermann, J. Nucl. Mater. 278 (2000) 85.
[3] H. Glasbrenner, J. Konys, G. Mueller, A. Rusanov, J. Nucl. Mater. 296 (2001) 237.
[4] C. Fazio, G. Benamati, C. Martini, G. Palombarini, J. Nucl. Mater. 296 (2001) 243.
[5] G. Benamati, C. Fazio, H. Piankova, A. Rusanov, J. Nucl. Mater. 301 (2002) 23.
[6] Ph. Deloffre, A. Terlain, F. Barbier, J. Nucl. Mater. 301 (2002) 35.
[7] G. Müller, A. Heinzel, J. Konys, G. Schumacher, A. Weisenburger, F. Zimmermann, V. Engelko, A. Rusanov, V. Markov, J. Nucl. Mater. 301 (2002) 40.
[8] R. Ballinger, J. Lim, E. Loewen, in: Proceedings of the 11th International Conference on Nuclear Engineering, Tokyo, No. ICONE11-36531, 2003.
[9] M. Takahashi, H. Sekimoto, K. Ishikawa, N. Sawada, T. Suzuki, K. Hata, S. Yoshida, S. Qiu, T. Yano, M. Imai, in: Proceedings of the11th International Conference on Nuclear Engineering, Arlington, Virginia, No. ICONE10-22226, 2002.
[10] Y. Kurata, M. Futakawa, K. Kikuchi, S. Saito, T. Osugi, J. Nucl. Mater. 301 (2002) 28.
[11] T. Furukawa, K. Aoto, G. Müller, G. Schumacher, A. Weisenburger, A. Heinzel, F. Zimmermann, J. Nucl. Sci. Technol. 41 (3) (2004) 265.
[12] T. Furukawa, G. Müller, G. Schumacher, A. Weisenburger, A. Heinzel, K. Aoto, J. Nucl. Mater. 335 (2004) 189.
[13] Ph. Deloffre, F. Balbaud-Célérier, A. Terlain, J. Nucl. Mater. 335 (2004) 180.
[14] G. Müller, A. Heinzel, G. Schumacher, A. Weisenburger, J. Nucl. Mater. 321 (2003) 256.
[15] D. Risold, B. Hallstedt, L.J. Gaukler, H.L. Lukas, S.G. Fries, J. Phase Equilib. 16 (1995) 223.
[16] B.F. Gromov, Y.I. Orlov, P.N. Martynov, V.A. Gulevski, in: Proceedings of the Conference HLMC 98, Obninsk: SSC RF-IPPE, vol. 1, 1999, p. 87.
[17] F.D. Richardson, J.H.E. Jeffes, J. Iron Steel Inst. 160 (1948) 261.
[18] K. Hauffe, Oxidation of Metals, Plenum, 1965.
[19] A.S. Khanna, High Temperature Oxidation and Corrosion, ASM International, 2002.
[20] J. Töpfer, S. Aggarwal, R. Dieckmann, Solid State Ionics 81 (1995) 251.
[21] T. Furukawa, J. Konys, G. Müller, K. Aoto, in: Proceedings of the 13th International Conference on Nuclear Engineering, Beijing, No. ICONE13-50145, 2005.